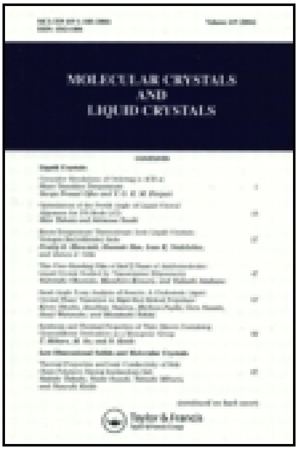

Molecular Crystals and Liquid Crystals

Publication details, including instructions for authors and subscription information:
http://www.tandfonline.com/loi/gmcl20

Effect of Different Dopants on Polymer Cholesteric Liquid Crystal Flakes

Anka Trajkovska Petkoska [a] & Stephen D. Jacobs [a] [b]

[a] Department of Chemical Engineering, University of Rochester, Rochester, New York, U.S.A

[b] Laboratory for Laser Energetics, University of Rochester, Rochester, New York, U.S.A

Version of record first published: 30 Jan 2009

To cite this article: Anka Trajkovska Petkoska & Stephen D. Jacobs (2008): Effect of Different Dopants on Polymer Cholesteric Liquid Crystal Flakes, Molecular Crystals and Liquid Crystals, 495:1, 334/[686]-347/[699]

To link to this article: http://dx.doi.org/10.1080/15421400802430471

Mol. Cryst. Liq. Cryst., Vol. 495, pp. 334/[686]–347/[699], 2008
Copyright © Taylor & Francis Group, LLC
ISSN: 1542-1406 print/1563-5287 online
DOI: 10.1080/15421400802430471

Taylor & Francis
Taylor & Francis Group

Effect of Different Dopants on Polymer Cholesteric Liquid Crystal Flakes

Anka Trajkovska Petkoska[1] **and Stephen D. Jacobs**[1,2]
[1]Department of Chemical Engineering, University of Rochester, Rochester, New York, U.S.A
[2]Laboratory for Laser Energetics, University of Rochester, Rochester, New York, U.S.A

Two types of dopants are incorporated into polymer cholesteric liquid crystal (PCLC) materials to change their dielectric properties. Conductive dopants consisting of either carbon-based or metallic particles show large increases in composite conductivity with percolation thresholds of from 0.4 vol% to 30 vol%, depending on the size and shape of the dopant particles. Inorganic insulating dopants change the dielectric constant from 2 (neat PCLC) to <10 at dopant levels of ~30 vol%, accompanied by an increase in density. These composites offer opportunities for use of PCLC's as particles or flakes in reflective displays.

Keywords: conductivity; dielectric constant; dopants; particle displays; percolation threshold; polymer cholesteric liquid crystals

1. INTRODUCTION

In this work we consider dopants that can alter the dielectric properties of polymer cholesteric liquid crystals (PCLC's) [1,2]. We use PCLC material to manufacture shaped PCLC flakes [3,4]. PCLC flakes are important for their electro-optical (EO) behavior in flexible particle display applications like electronic paper [5,6]. Doping extends flake EO response to the dc drive [7].

The authors thank K. L. Marshall and Dr. T. Z. Kosc (Laboratory for Laser Energetics) for suggestions regarding this manuscript. The authors also acknowledge K. Hasman and Jessica DeGroote (The Institute of Optics, University of Rochester) for sample preparation and the acquisition of SEM images, respectively. Author ATP acknowledges the Laboratory for Laser Energetics at the University of Rochester for Horton Fellowship support.

Address correspondence to Stephen D. Jacobs, Laboratory for Laser Energetics, University of Rochester, 240 East River Road, Rochester, New York 14623, U.S.A. E-mail: sjac@lle.rochester.edu

A variety of particulate substances, like carbon-based, metallic, etc., can be used as dopants or fillers in polymers [8–13]. Particle *dopants* can vary in both shape (e.g., spherical, fiber-like, tubes, or even flake platelets) and size (from nano to micro). They form heterogeneous composites with unique properties. These composites exhibit improvements over those of the neat host material in terms of mechanical, electrical, optical, and thermal properties [8,12–14], tailoring them to different applications.

Conductive dopants cause an insulating-to-conducting transition [8] of the polymer composite. This occurs when the dopant concentration exceeds a critical value known as the percolation threshold (PT) [9,15,16]. PT is characterized by a sharp jump in the conductivity by many orders of magnitude. The concentration at which PT occurs depends on many factors: the nature of both the polymer host and the dopant; the composite porosity; dopant dispersion and alignment; chemical interactions; processing method; and the presence of surfactants, ionic salts, and shear force [9,15]. Generally, smaller PT values are desirable and can be achieved with elongated dopants (higher geometric aspect ratio) [17–19] compared to spherical ones [17,20]. Also, better dopant dispersion contributes to lowering PT [11,21].

Different percolation models interpret the behavior of the electrical conductivity of different mixtures: statistical, geometrical, thermodynamic, and structure oriented [19]. The classical statistical model explanation of the conductivity of a composite (mixture), σ_m, is due to the existence of "infinite clusters" of connected conducting particles (forming a three-dimensional conductive network over the entire sample) and is given with a power-law dependence [11,16,17,21,22]:

$$\sigma_m \approx (p - p_c)^t \quad \text{for } p > p_c, \tag{1}$$

where p is the volume fraction of the filler, p_c is the filler's critical volume fraction at the percolation threshold ($p_c \cong \text{PT}$), and t is the conductivity exponent determining the increase of the conductivity above the PT (usually $t = 1.5$ to 2). The dielectric constant of the composite ε_m is also affected by the dopant. Itexhibits a power-law behavior [16,22]:

$$\varepsilon_m = (p_c - p)^{-s} \quad \text{for } p < p_c \tag{2}$$

where s is the dielectric permittivity critical exponent (usually reported to have values of $|s| = 0.7$ to 0.9, absolute values) [9,10,20]. Statistical theory gives a good description of PT, and the critical volume fraction for percolation is calculated to be $\sim$16 vol%.

Discrepancies, however, are observed between critical parameters like p_c, t, s, and the experimental results. Departures from the universal values for t and s have been reported; for example, the value of t can be $t = 1$ to 7 for elongated particles [11,17,21] or even much smaller $t < 1$ [16]. Discrepancies may be due to the fact that the statistical theory does not cover the properties of the polymer host (viscosity, surface tension), polymer/dopant chemical interactions, or dopant geometry. "Continuous chains" of particles do not always exist in conductive composites as the theory assumes; discontinuities (e.g., thin polymer barrier layers) may occur between the particles. In this case, the composites can exhibit a semiconducting or conducting character with conduction occurring through a "tunneling" effect and/or a "hopping" of charge carriers among neighboring particles (non-universal percolation) [17,23,24]. Consequently, much lower percolation thresholds are observed (even lower than 0.1 vol%) [18,23] than the classical statistical theory would predict.

Polymer-ceramic materials [25,26] or polymers doped with $BaTiO_3$ offer the potential of having a high dielectric constant due to the ceramic. The dielectric properties depend primarily on the content, size, and distribution of the dopant particles, and processing techniques (e.g., incorporation of pores and/or voids in the material). When very high dopant concentrations (e.g., 51 vol% [26]) are required to increase the dielectric constant of the composite, processing can become more difficult; other properties (e.g., optical) may also be disrupted. Another problem that usually arises for $BaTiO_3$, in powder form, is the difficulty in measuring the true value for the dielectric constant. There is no direct methodology. Usually, a measured value for the bulk solid is used. The particle (grain) size of polycrystalline $BaTiO_3$ is very important for determining its dielectric constant. Literature values vary from 100 to 600 (for grain size $<0.7\,\mu m$) [27] to $\sim$5000 (for grain size between 0.7 and 1 μm) [28,29]. TiO_2/polymer composites are reported to exhibit improved mechanical properties, as well as increased dielectric constants; however, nano-sized TiO_2 has a larger effect than micron-sized TiO_2 [30] on mechanical properties in TiO_2/polymers.

Many equations exist that can be used to calculate the dielectric constant of doped polymer mixtures. The *logarithmic* equation (or *Lichtenecker–Rother* equation) [26,27] is commonly used to predict the dielectric constant of statistical/chaotic composites. It is given as:

$$\log \varepsilon_m = f_1 \log \varepsilon_1 + f_2 \log \varepsilon_2, \tag{3}$$

where ε_m is the dielectric constant of the mixture and ε_1, ε_2, f_1, and f_2 are the dielectric constants and volume fractions of each component (1 refers to the polymer host and 2 for dopant).

2. EXPERIMENTAL

2.1. Materials

Table 1 and the text that follows briefly describe the dopants studied in this work, which are grouped as follows: (1) carbon-based dopants (conductive), (2) metal-based dopants (conductive), and (3) inorganic dopants (nonconductive, but with a high dielectric constant).

(1) Carbon-based dopants can be carbon black, carbon fibers, or carbon nanotubes. *Carbon black* (CB) consists of spherical-shaped, nano-sized particles that usually aggregate in agglomerates with two types of structure [17,31,32]. More spherical-like and compact aggregates (or isolated CB particle) have "lower"

TABLE 1 Dopants Used for PCLC Composites (see text for a discussion of abbreviations)

Dopant	Particle size*	PT (vol%)	Conductivity (1 kHz) at PT [S/m]	Dielectric constant (10 kHz) at PT or at vol%
Neat PCLC (no dopant)	–	–	$\sim 1 \times 10^{-9}$	2.1
1) C-based				
CB VPA	17 nm	2	1×10^{-5}	10
CB M	75 nm	6	1×10^{-5}	10
SWNT-1	1.4 × 2 to 5 μm	0.7	1×10^{-6}	5
SWNT-2	1.1 nm × 0.5 to 100 μm	0.4	1×10^{-6}	2.2
MWNT	10 to 20 nm × 0.5 to 200 μm	0.8	$\sim 1 \times 10^{-3}$	10
2) Metal-based				
CI-HQ	1.1 μm	20	1	–
ITO	3.38 μm	25	$\sim 1 \times 10^{-4}$	5
Al flakes	12 μm	30	$\sim 1 \times 10^{-2}$	20
3) Inorganic				
$BaTiO_3$-1	70 nm	–	–	7.7 (27.0)
$BaTiO_3$-2	1 to 1.1 μm	–	–	6.1 (32.0)
$BaTiO_3$-3	1.3 to 1.8 μm	–	–	5.8 (27.0)
TiO_2-1	30 nm	–	–	5.2 (54.4)
TiO_2-1	10 nm × 40 nm	–	–	7.5 (22.0)

*Primary average particle dimensions.

structure with less pores and few voids (less absorption of dibutyl phthalate-DBP oil, which is an effective measure of CB structure [31]). More-elongated, branched, and chained aggregates form a "high" structure that is more porous and has a large effective volume and a high DBP value. Different loading levels of CB in polymers are reported that exhibit percolation thresholds from <1 vol% to 39 vol%. The two types of carbon blacks, Vulcan PA90 (VPA) and Monarch M120 (M), used in this work (obtained from Cabot Corporation, Billerica, MA) have different morphologies: CB VPA has a smaller particle size with a high surface area, "high" structure (forms elongated, branched, and chained aggregates), and high DBP [31] compared to CB M [32]. Knowing these properties of the CB powders, it is expected that CB VPA will give a higher conductivity as a dopant in PCLC at a lower concentration (low PT).

Since their discovery, *carbon nanotubes* (CNT) and their unique properties [33] have attracted the attention of many researchers for use as dopants. They can be single-walled carbon nanotubes (SWNT's), double-walled carbon nanotubes (DWNT's), or multi-walled carbon nanotubes (MWNT's). Low PT's are beneficial since small dopant concentrations leave other polymer properties (like selective reflection in PCLC [34] unaffected. We use two types of SWNT's (products by: CarboLex Inc., Lexington, KY, AP – grade, and Sigma Aldich, cat. #636797), and one type of MWNT's (product of Sigma Aldrich, cat. #636525).

(2) Metal-based dopants with different particle sizes are chosen. Usually metal dopants in polymers show a percolation threshold-type behavior, but this occurs at relatively high dopant loadings [20]. We use carbonyl iron HQ (CI-HQ, product of BASF Corp.), indium tin oxide (ITO, Sigma Aldrich product cat. #49468-2), and aluminum (Al) flakes (Starbrite 4102-EAC, Silberline, Tamaqua, PA) for this work.

(3) The inorganic dopants considered for this work consist of three types of $BaTiO_3$ and two of TiO_2 with different sizes and shapes. [Using a scanning electron microscope (SEM), we have determined that these powders are highly aggregated.] We choose nano- and micro-sized $BaTiO_3$ powders, knowing that the dielectric constant of this dopant varies substantially with the particle size [29], (products by: Sigma Aldrich cat. #46763-4; GFS Chemicals cat. #A0882; and Across Organics cat. #19685000). Two types of rutile TiO_2 are studied: one of them, TiO_2-1, consists of particles with a spherical shape (product of Marketech International, Inc., Port Townsend, WA), while TiO_2-2 particles are needle

shaped (Nanostructured & Amorphous Materials, Inc., Los Alamos, NM, stock #5480MR).

2.2. Manufacture and Measurement

Pellets made from pure dopant powder are not easily prepared because of their high melting temperatures or their inability to be compressed into pellets. Therefore, doped disks (plates or pellets) made from PCLC's (product of Wacker–Chemie GmbH, Munich, Germany) and a particular dopant are prepared to determine the dielectric properties of the composite [1,2]. For each system (PCLC/dopant), approximately 10 or more samples (with different concentrations) are manufactured to be ~2 cm in diameter and ~0.5 mm in thickness. A "thin filmmaker tool" with controlled heating and pressure is used (constant-thickness filmmaker and thin-film–making kits are products of International Crystal Laboratories, Garfield, NJ). First, target compositions with specified amounts of PCLC's and dopant material are measured, ground by mortar and pestle, and mixed well in a small vibrational capsule. The mixed powders are melted to 130°C under a pressure of ~4000 kg for ~5 min and then cooled down to room temperature. The disks are placed in an impedance/gain phase analyzer for measurement (Solartron 1260, impedance/gain phase analyzer is manufactured by Solartron Analytical, Unit B1 Armstrong Mall, Farnborough, Hampshire, England, GU14 ONR). The output of this instrument is converted to resistance R and capacitance C as a function of frequency. From these data, the conductivity and dielectric constant for each dopant/PCLC composite are calculated [35,36].

3. RESULTS AND DISCUSSION

3.1. Carbon-Based Dopants

We compare two types of CB's as PCLC dopants in this work. Figure 1(a) shows some SEM pictures of 5-vol% CB VPA-doped PCLC flakes. The clumps or CB aggregates (white in the image) are ~200 to 300 nm in size. For reference, the half pitch for the selective reflection structure shown in the SEM picture for this green PCLC composition is $p/2 = 170\,\text{nm}$. Figure 1(b) shows the increase in conductivity of PCLC/CB VPA composite as a function of dopant level (conductivity here and in later sections of the text is reported at 1 kHz, which for these measurements is commonly considered to be the same or close to the dc conductivity [16,37], while Figure 1(c) shows the dielectric

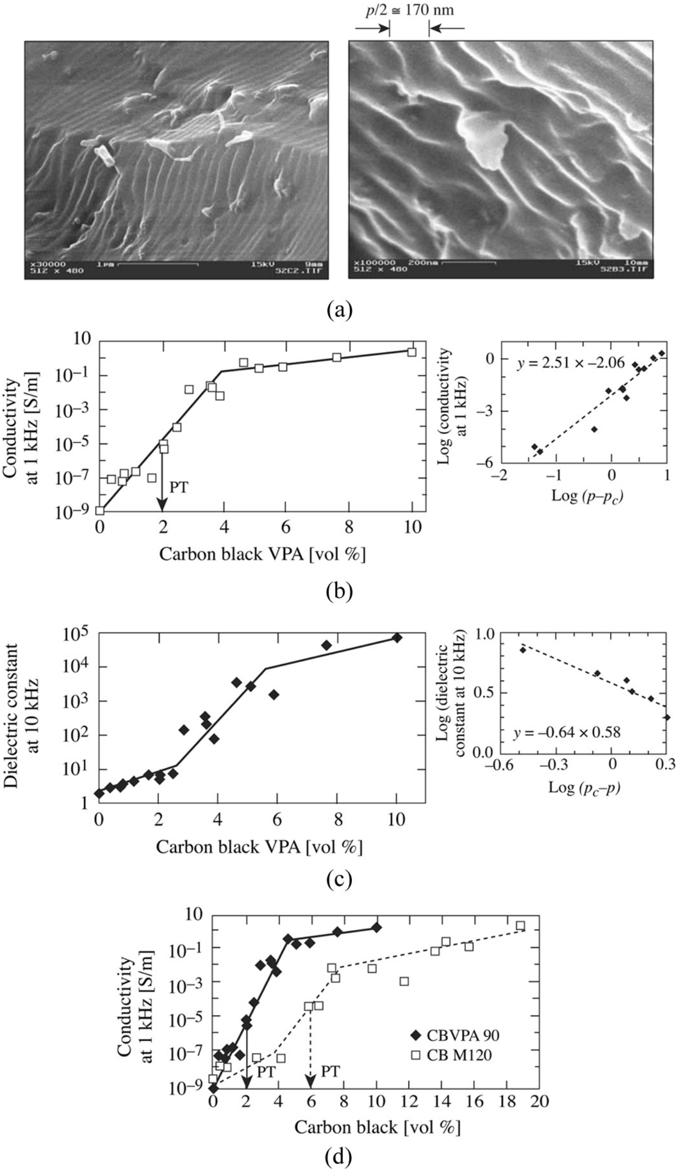

FIGURE 1 (a) SEM pictures of 5-vol% CB VPA (white in the image) in PCLC. (b) Conductivity of CB VPA/PCLC composites as a function of dopant level [Inset: power law—Eq. (1)]. (c) Dielectric constant of CB VPA/PCLC composites as a function of dopant level [Inset: power law—Eq. (2)]. (d) Comparison of conductivity for PCLC doped with CB VPA and CB M and their percolation thresholds. (Lines are drawn to guide the eye.)

constant of PCLC composite as a function of dopant concentration. Figure 1(d) compares both carbon blacks: CB VPA shows lower PT than CB M, as expected, due to the difference in its morphology.

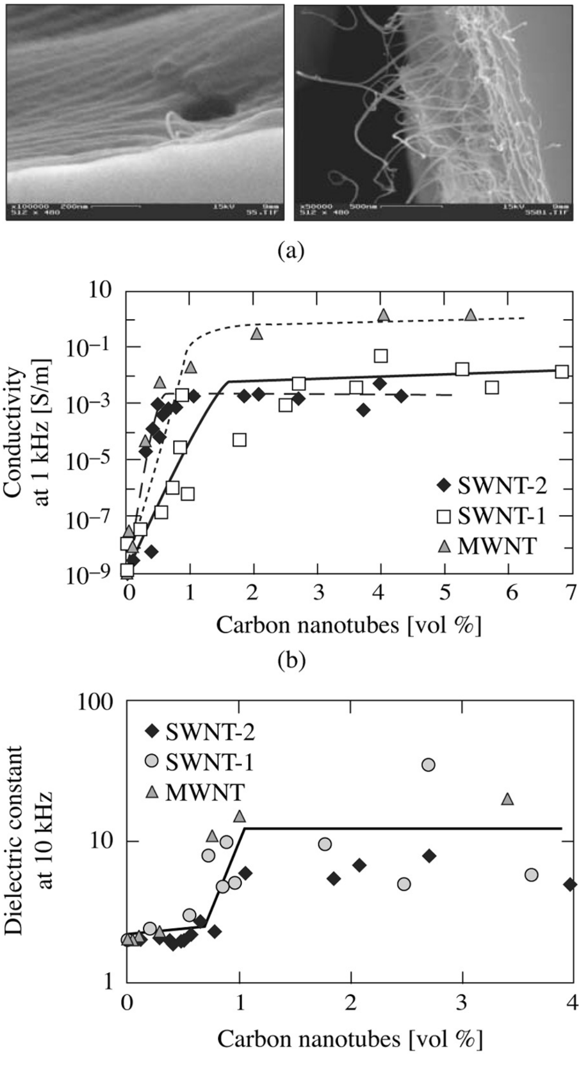

(a)

(b)

(c)

FIGURE 2 (a) SEM pictures of 1.2-vol%, SWNT-1 doped PCLC (left side-view from the top, right side-side view). (b) Comparison of conductivities and (c) comparison of dielectric constants for PCLC composites doped with SWNT-1, SWNT-2, and MWNT (lines are drawn to guide the eye).

Percolation threshold (PT) is determined by measuring σ and ε as a function of doping level for a series of PCLC doped disks. Using the data in Figure 1(b), the calculation is carried out in an iterative manner by first examining the behavior of σ as a function of doping. A several trial p_c values (PT) are selected as midpoints, and by using Eqs. (1) and (2), two graphs are generated: $\log(\sigma)$ versus $\log(p - p_c)$ and $\log(\varepsilon)$ versus $\log(p_c - p)$, giving t and $|s|$ values, respectively [insets in Figs. 1(b) and 1(c)]. The p_c trial value that gives the highest correlation factor (R^2) value for t and $|s|$ (in this case it is $p_c = 2$) was chosen as PT. For all other conductive dopants shown in this paper, the same procedure for determining the PT is used.

The three types of carbon nanotubes used as dopants in PCLC are compared below. Figure 2(a) shows two SEM pictures of 1.2-vol % SWNT-1 doped into a shaped PCLC flake. The first picture (left side) gives a view from the top of a doped shaped flake. The other picture shows a higher doping level of nanotubes that was achieved in the near surface of a flake looking edge-on. Figure 2(b) plots the increase in conductivity (at 1 kHz) for PCLC disks doped with SWNT-1, SWNT-2, and MWNT. PT's are determined as 0.70, 0.37, and 0.80 vol% for SWNT-1, SWNT-2, and MWNT, respectively. Figure 2(c) shows an increase in dielectric constant for PCLC composites doped with different CNT's.

3.2. Metal-Based Dopants

Generally, metal-based dopants show high percolation thresholds. CI-HQ increases the conductivity of PCLC/CI-HQ composites by nine

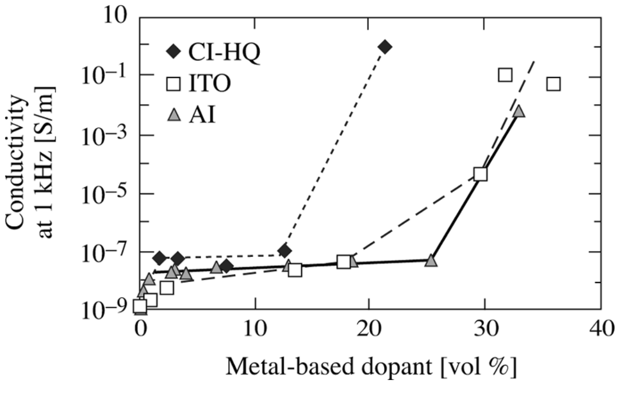

FIGURE 3 Conductivity of PCLC composites doped with CI-HQ, ITO, and Al flakes. (Lines are drawn to guide the eye.).

orders of magnitude at a dopant level of ~20 vol% (PT). ITO as a dopant increases the conductivity of ITO/PCLC composites by eight orders of magnitude at doping levels of ~25 to 30 vol%. PT for Al flakes is at 30 vol% or higher. A pure Al disk pressed from Al flakes gives a conductivity that is ten orders of magnitude higher (not shown) than that for neat PCLC. All metal-based dopants are compared in Figure 3.

Conductivity data for all carbon-based and metal-based dopants are summarized in Figure 4. There are two types of behavior: For carbon-based particles, PT drops as shape anisotropy increases [Fig. 4(b)]. This has been observed in other polymer hosts [38]. For metal-based

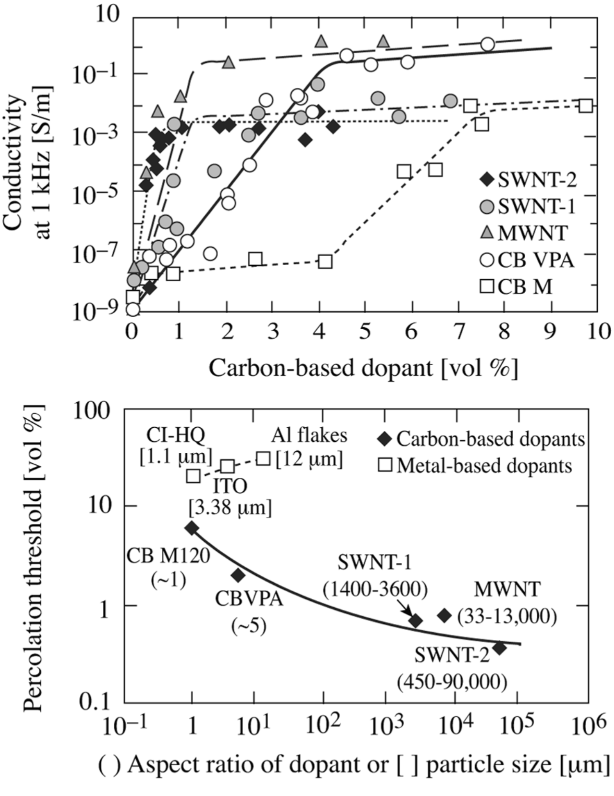

FIGURE 4 (a) Carbon-based dopants: comparison of conductivity at 1 kHz versus dopant concentration, (b) PT versus dopant average aspect ratio (range given in parentheses) or particle size (given in brackets). (Lines are drawn to guide the eye.).

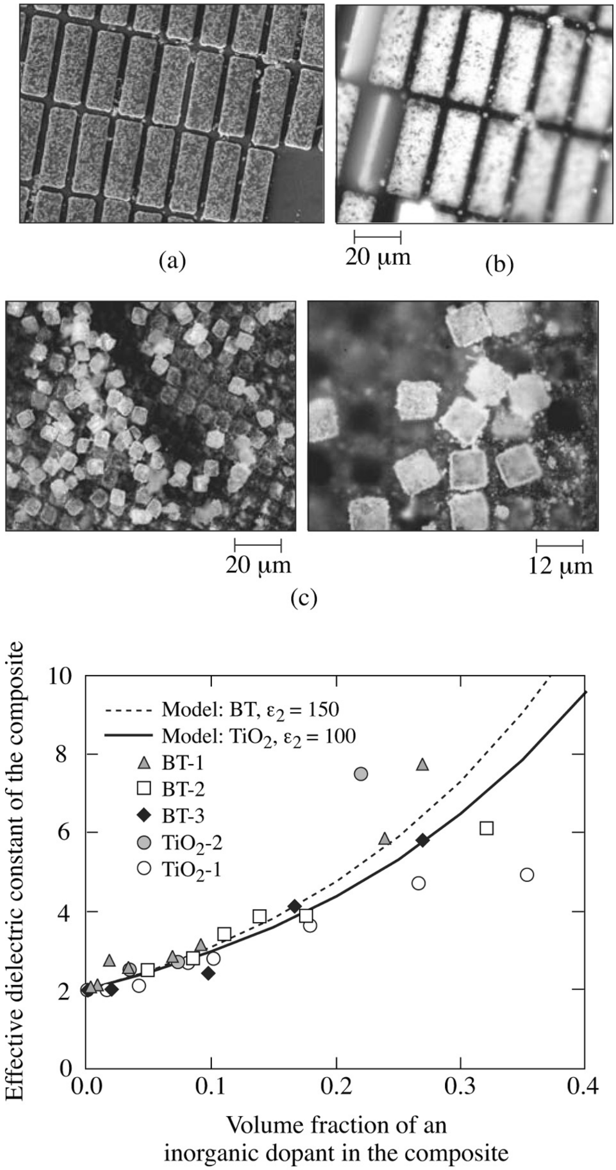

FIGURE 5 (a) SEM image of $BaTiO_3$-1–doped, PCLC rectangular flakes. (b) POM image of $BaTiO_3$-1–doped PCLC rectangular flakes. (c) POM images of TiO_2-1–doped square PCLC flakes. d) Measured dielectric constants (10 kHz) for PCLC composites with all inorganic dopants $BaTiO_3$-(1, 2, 3) and TiO_2-(1, 2) compared to theoretical calculations using the logarithmic equation.

particles with little shape anisotropy, PT increases with increasing particle size (CI-HQ, ITO, Al flakes) [Fig. 4(b)].

3.3. Inorganic Dopants

All inorganic dopants used in this paper show a similar effect on PCLC dielectric properties. They increase the dielectric constant of the composite at relatively high dopant loadings. Figure 5(a) shows an SEM image of 20-vol%, $BaTiO_3$-1–doped PCLC rectangular-shaped flakes, while Figure 5(b) shows polarizing optical microscope (POM) images of 20-vol% $BaTiO_3$ (1) doped PCLC flakes. High $BaTiO_3$ concentrations in PCLC disrupt the selective reflection. Figure 5(c) shows POM pictures of 20-vol%, TiO_2-doped flakes. These particles also exhibit a reduction in the quality of selective reflection.

Figure 5(d) compares the effect of all $BaTiO_3$ and TiO_2 inorganic dopants in PCLC's. Generally, all show an increase in composite dielectric constant up to ten at very high dopant levels, e.g., ≥ 20 vol%. Higher dopant concentrations in PCLC's are difficult to achieve. A logarithmic Eq. (3) for the effective dielectric constant of the composite agrees well with our experimental data. The main problem here is choosing an appropriate value of the dopant dielectric constant to use in the model. In our case PCLC/$BaTiO_3$ composites are well fitted with the log equation when $\varepsilon(BaTiO_3)$ is ~ 150 (vendor supplied value: 150 for $BaTiO_3$-1), while for TiO_2 we use $\varepsilon(TiO_2) \sim 100$. Deviations between the experimental data and theoretical calculations can also be due to (a) the quality of dopant dispersion in the polymer matrix, (b) agglomeration, and/or (c) incorporation of air voids/pores inside the samples, which can drastically decrease the ε_m.

4. CONCLUSION

In conclusion, conductive particles like carbon- and metal-based dopants show a percolation threshold behavior in the PCLC host, increasing the conductivity of the composite by several orders of magnitude when the PT is reached. We believe that we can decrease the dopant level in PCLC flakes, but maintain high levels of conductivity, by better and more uniformly dispersing the particles, e.g., by using a solvent that first dissolves the host polymer, and then by sonicating together with the dispersed dopant. Alternatively, use of a surfactant or ionic salt could improve separation of dopant particles within the host matrix.

The tested inorganic dopants show similar behavior. All three types of $BaTiO_3$ have almost the same effect on the PCLC composite dielectric constant, regardless of the particle size. TiO_2-2 with needle-like particles are more effective than the spherical TiO_2-1 particles. It is possible that TiO_2-1 consists of some anatase phase material that would lower the dielectric constant compared to TiO_2-2. However, inorganic dopants are of less interest for our intended particle display application for doped PCLC flakes since the increase in dielectric constant of PCLC composites made with them is modest, even at high concentrations. At these high concentrations, the selective reflection of our PCLC flakes is substantially disrupted. It is possible that our use of a layer of doped PCLC sandwiched between neat PCLC layers would offer some advantages.

REFERENCES

[1] Trajkovska-Petkoska, A. (2007). Ph.D. thesis, University of Rochester, Rochester, NY.
[2] Trajkovska-Petkoska, A., Jacobs, S. D., Marshall, K. L., & Kosc, T. Z. *U.S. Patent Application* Serial No. 11/230,059 (filed 14 January 2006).
[3] Trajkovska-Petkoska, A., Jacobs, S. D., Kosc, T. Z., & Marshall, K. L. (2007). *U.S. Patent* 7,238,316 B2.
[4] Trajkovska-Petkoska, A., Varshneya, R., Kosc, T. Z., Marshall, K. L., & Jacobs, S. D. (2004). *Adv. Funct. Mater.*, *15*, 217.
[5] Kosc, T. Z., Marshall, K. L., Trajkovska-Petkoska, A., Hasman, K., Coon, C. J., Babcock, G. V., Howe, R., Leitch, M., & Jacobs, S. D. (2007). Presented at SPIE Photonics West, San Jose, CA, January 20–25.
[6] Marshall, K. L., Trajkovska-Petkoska, A., Kosc, T. Z., & Jacobs, S. D. (2006). Presented at USDC's Fifth Annual Flexible Displays and Microelectronics Conference, Phoenix, AZ, February 6–9.
[7] Trajkovska-Petkoska, A., Kosc, T. Z., Marshall, K. L., Hasman, K., & Jacobs, S. D. (2008). *J. Appl. Phys.*, *103*, 094907.
[8] Maaroufi, A., Haboubi, K., Almarti, A. El., & Carmona, F. (2004). *J. Mater. Sci.*, *39*, 265.
[9] Carmona, F. (1989). *Physica A*, *157*, 461.
[10] Zois, H., Mamunya, Y. P., & Apekis, L. (2003). *Macromol. Symp.*, *198*, 461.
[11] Sandler, J. K. W., Kirk, J. E., Kinloch, I. A., Shaffer, M. S. P., & Windle, A. H. (2003). *Polymer*, *44*, 5893.
[12] Breuer, O. & Sundararaj, U. (2004). *Polymer Compos.*, *25*, 630.
[13] Moniruzzaman, M. & Winey, K. I. (2006). *Macromolecules*, *39*, 5194.
[14] Jiang, X., Bin, Y., & Matsuo, M. (2005). *Polymer*, *46*, 7418.
[15] Schueler, R., Petermann, J., Schulte, K., & Wentzel, H.-P. (1997). *J. Appl. Polym. Sci.*, *63*, 1741.
[16] Flandin, L., Prasse, T., Schueler, R., Schulte, K., Bauhofer, W., & Cavaille, J.-Y. (1999). *Phys. Rev. B*, *59*, 14,349.
[17] Balberg, I. (2002). *Carbon*, *40*, 139.
[18] Martin, C. A., Sandler, J. K. W., Shaffer, M. S. P., Schwarz, M.-K., Bauhofer, W., Schulte, K., & Windle, A. H. (2004). *Compos. Sci. Technol.*, *64*, 2309.
[19] Lux, F. (1993). *J. Mater. Sci.*, *28*, 285.
[20] Zois, H., Apekis, L., & Mamunya, Y. P. (2003). *Macromol. Symp.*, *194*, 351.

[21] Tchmutin, I. A., Ponomarenko, A. T., Krinichnaya, E. P., Kozub, G. I., & Efimov, O. N. (2003). *Carbon*, *41*, 1391.

[22] Zois, H., Apekis, L., & Omastová, M. (2001). *Macromol. Symp.*, *170*, 249.

[23] Kilbride, B. E., Coleman, J. N., Fraysse, J., Fournet, P., Cadek, M., Drury, A., Hutzler, S., Roth, S., & Blau, W. J. (2002). *J. Appl. Phys.*, *92*, 4024.

[24] Balberg, I. (1987). *Phys. Rev. Lett.*, *59*, 1305.

[25] Popielarz, R., Chiang, C. K., Nozaki, R., & Obrzut, J. (2001). *Macromolecules*, *34*, 5910.

[26] Chiang, C. K. & Popielarz, R. (2002). *Ferroelectrics*, *275*, 1.

[27] Cho, S.-D., Lee, S.-Y., Hyun, J.-G., & Paik, K.-W. (2005). *J. Mater. Sci.*, *16*, 77.

[28] Buscaglia, M. T., Buscaglia, V., Viviani, M., Petzelt, J., Savinov, M., Mitoseriu, L., Testino, A., Nanni, P., Harnagea, C., Zhao, Z., & Nygren, M. (2004). *Nanotechnology*, *15*, 1113.

[29] Shaw, T. M., Trolier-McKinstry, S., & McIntyre, P. C. (2000). *Annu. Rev. Mater. Res.*, *30*, 263.

[30] Ng, C. B., Schadler, L. S., & Siegel, R. W. (1999). *Nanostruct. Mater.*, *12*, 507.

[31] Foster, J. K. (1991). *2-nd International Exhibition of Paint Industry Suppliers*, Sao Paulo: Brazil.

[32] Heithaus, M. F. & Foster, J. K. (1995). *4-th International Exhibition of Paint Industry Suppliers*, Sao Paulo: Brazil.

[33] Dresselhaus, M. S., Dresselhaus, G., & Jorio, A. (2004). *Annu. Rev. Mater. Res.*, *34*, 247.

[34] Fergason, J. L. (1966). *Mol. Cryst.*, *1966*, *1*, 293.

[35] Riad, A. S., Korayem, M. T., & Abdel-Malik, T. G. (1999). *Physica B*, *270*, 140.

[36] Ye, H., Sun, C. Q., Huang, H., & Hing, P. (2001). *Appl. Phys. Lett.*, *78*, 1826.

[37] Connor, M. T., Roy, S., Ezquerra, T. A., Calleja, F. J. B. (1998). *Phys. Rev. B*, *57*, 2286.

[38] Collins, P. & Hagerstrom, J. (2002). *Hyperion Catalysis International*, Cambridge, MA 02138 (technical notes: www.fibrils.com/articles2.htm).